Investigation of AE Generation from Fatigue Cracks for Structural Health Monitoring in 2014 Aluminium Alloy

D. GAGAR, P. IRVING, P. FOOTE and J. MCFEAT

ABSTRACT

Acoustic Emission (AE) generation in 2014 aluminium sheets is investigated in this study. Fatigue tests were conducted with samples under constant amplitude loading, monitoring the rates of AE signals generated during fatigue crack propagation. The load output from the test machine was correlated with recorded AE signals as a means for AE source characterisation. The results showed 3 stages in AE generation with the vast majority of AE signals recorded occurring around or below the mean cyclic load from the emergence of crack to the period just before sample failure where they appeared across the entire loading range.

INTRODUCTION

The Acoustic Emission (AE) technique is capable of detecting and locating fatigue cracks occurring in metallic structures via generation of acoustic waves. Crack location is achieved via Time of Flight (TOF) analysis of AE signals monitored by an array of sensors. AE signals generated during fatigue crack growth in metallic materials are variously attributed to processes associated with crack extension[1; 2], plasticity at the crack tip resulting in failure of local second phase particles [3 - 5] and fretting of crack surfaces [6]. Even though the TOF technique is well established, without a complete understanding of the circumstances of AE production and the factors which control it, AE cannot be regarded as a credible technique for continuous health monitoring of structures.

Daniel Gagar, Phil Irving, Cranfield University Centre for IVHM, Cranfield, Bedfordshire, UK MK43 0FQ
Peter Foote, BAE Systems, ATC-Sowerby, FTC 267, PO Box 5, Filton, Bristol, UK
Jim McFeat, BAE Systems, Warton Aerodrome, Lancashire, UK. W427D

Service application of structural health monitoring for damage location and characterisation will require validation and verification of performance. This may be defined in terms of sensitivity in detecting AE signals produced from damage sites and also in terms of accuracy in damage location. The former can be quantified via measurements leading to Probability of Detection (POD) and the latter with Probability of Location (POL) curves. The work in this paper investigates factors controlling generation of AE and investigates the role of crack tip stress intensity and crack length in determining AE emission rates.

EXPERIMENTS

AE activity was measured during fatigue crack propagation in Single Edge Notch (SEN) specimens of 2 mm thick 2014 T6 aluminium. The test samples were 250 mm wide and 530 mm long. A 10 mm deep notch was placed at the sample edge, midway along the length. The fatigue crack initiated at the notch root and propagated perpendicular to the applied load across the sample width. One side of each sample was polished and marked with scribes at 1 mm intervals to facilitate monitoring of the crack length. A digital video system was used to capture images of the crack tip, with an appended timestamp, as it progressed across the sample. Image frames were recorded at intervals of 600 cycles and were used in post-test analysis to determine crack length to an accuracy of ± 0.1 mm. Measurements of crack length are inclusive of the crack-initiating notch length.

Samples were subjected to constant amplitude sinusoidal loading at 2 Hz with a maximum stress of 58 MPa, stress range $\Delta\sigma$ of 52 MPa and an R ratio (min load/max load) of 0.1. Loads were recorded to an accuracy of 0.1%. The load channel of the test machine was monitored by the AE system via an analog input to enable cycle counting once a specified load threshold was crossed.

A Physical Acoustics 6-channel AE system (PCI2) equipped with WDI broad band piezoelectric sensors was used to record the AE data which was conditioned, filtered and amplified with a 40 dB_{AE} gain (0 dB_{AE} Ref. 1µV/sensor); sensors were coupled to the samples using Dow Corning RTV 3140 silicone rubber. The accompanying AEWin software package was used to control the acquisition setup and perform other signal processing functions.

AE Setup

A 1D (2 sensor) AE event location setup was used in all experiments with the sensor centres positioned on the sample vertical centre line, 70 mm and 130 mm on either side of the horizontal crack path. Exclusive detection of AE from the fatigue crack was ensured by implementing a timing filter based on time difference of AE arrival between sensors. This restricted AE acquisition and location to a defined region of the sensor array.

AE hits per mm of crack growth were calculated, together with kernel density distributions of the points in the load cycle at which emissions occurred with increased fatigue cycles and crack length. Kernel Density Estimation (KDE) is a non-parametric approach for estimating probability density function to assess multimodality of a data structure [7].

RESULTS

Three test trials were performed under constant amplitude loading. Figure 1 illustrates results from the first. Figure 1(a) shows that the first AE signals were detected at a crack length of about 12 mm, the hit rate increasing rapidly with crack growth, reaching a maximum of 6586 hits/mm at 15 mm where ΔK was 13 MPa $m^{1/2}$. Afterwards, the hit rate declined rapidly to near zero as crack growth progressed, with almost no emissions occurring from crack lengths of 17 mm to 60 mm. There was an increase in AE hit rate just before sample failure at crack lengths approaching 70 mm.

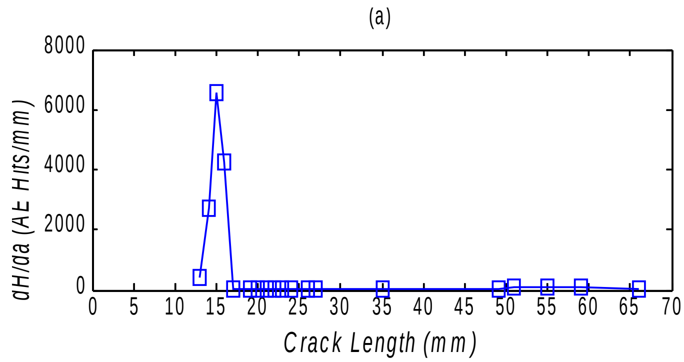

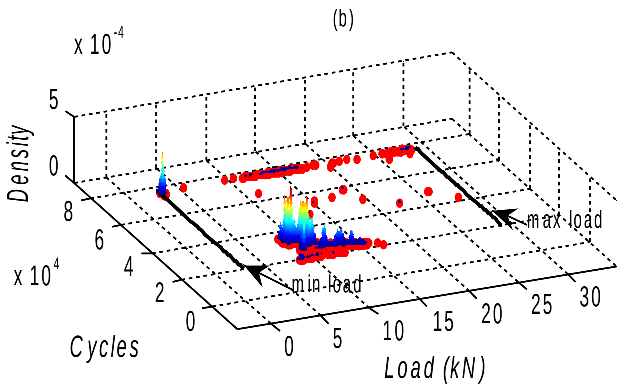

Figure 1: (a) Plot of AE hit rate versus crack length in Test 1 (b) Plot of AE hit density in loading cycles in Test 1, showing the points in the loading cycle where AE occurred.

Figure 1(b) shows a KDE plot of the AE hits occurring as a function of load in the loading cycle over the test duration. It can be seen that AE hits at the early part of the test occur just under the mean load, between 8 kN and 16 kN. In the period just prior to sample failure, the AE hits occurred throughout the entire loading range with its statistical mode at the about the minimum load.

Results from the second test are shown in Figure 2 and had very similar results to the previous one. The first AE signal was detected at a crack length of 11 mm, followed by a rapid increase in hit rate, reaching a maximum of 12000 hits/mm at 14 mm followed by a decline to near zero at 19 mm. Again there was a small increase in hit rate just before sample failure. Figure 2(b) shows that distributions of AE hits with applied load and cycles was again very similar to those found in test 1, with most emissions occurring at or around the mean cyclic load.

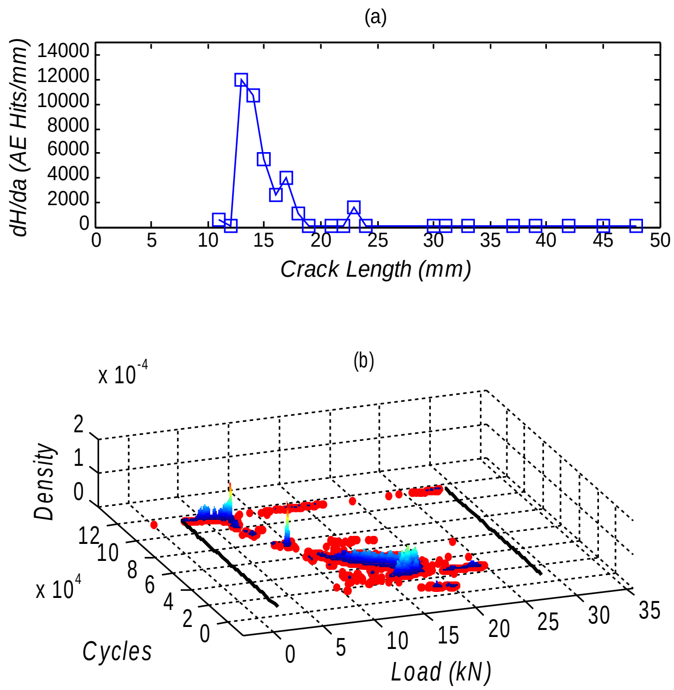

Figure 2: (a) Plot of AE hit rate versus crack length in Test 2 (b) Plot of AE hit density in loading cycles in Test 2, showing the points in the loading cycle where AE occurred.

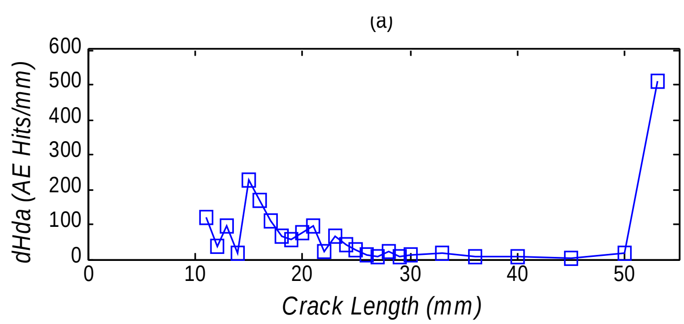

Figure 3: (a) Plot of AE hit rate versus crack length in Test 3

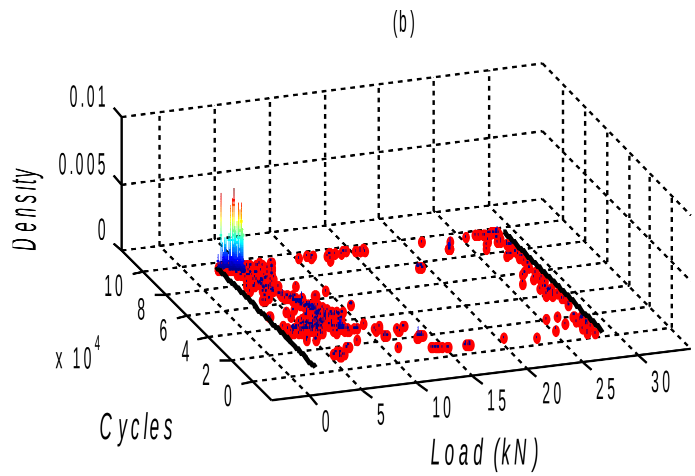

Figure 3(b): Plot of AE hit density in loading cycles in Test 2, showing the points in the loading cycle where AE occurred

Figure 3 illustrates the results from the third test trial. As in the previous two, a similar trend is observed in the increased rates of AE hits at crack lengths under 20 mm, followed by a decline to near zero and then an increase just before sample failure.

A comparison of the total number of AE hits recorded in all the tests conducted is shown in Table 1. It can be seen that the total number of AE hits varied greatly, with test 3 having only 15% of the emissions of test 2 with the most prolific emissions.

Table 1*: Total number of AE hits in each test*

Test	Number of AE Hits
1	15370
2	43190
3	6172

DISCUSSION

AE emissions observed in all tests had 3 stages. Stage 1 is characterised by increasing and then decreasing rates of AE activity at crack lengths of 12-19 mm, followed by small almost constant rates of AE emission in the next stage and an increase in AE just prior to failure in the final stage. Similar behaviour has been reported in other publications [8-10]. Han et al [8]. and Daniel et al. [9] both independently reported no emissions for 80% of the sample fatigue life in Q345 Steel and 2024-T3 Aluminium alloy respectively. Daniel et al. correlated the AE generated in Stage 1 to correspond with crack initiation, slow crack growth for those in Stage 2 and rapid crack growth for those in Stage 3.

There is no direct correspondence in the present work with the stages observed by Daniel, as all three stages in this work occurred during fatigue crack growth; AE hits produced during initiation as reported by Daniel et al. were negligible. The proportions of total crack growth life occupied by the three stages in this work are summarised in Table 2.

Table 2: *Summary of the stages in AE generation in terms of fatigue cycles, indicating proportions of their fatigue lives*

Test	Stage 1 (cycles) (%)	Stage 2 (cycles) (%)	Stage 3 (cycles) (%)
1	23369 – 35326 (15%)	35327 – 74887 (51%)	74888-77294 (3%)
2	17882 – 60101 (37%)	60102 – 109547 (43%)	109547-114865 (5%)
3	11751 – 51510 (41%)	51591 – 92988 (43%)	92989-96523 (4%)

The proportion of the first stage in AE generation, where the high emission rates occurred, varied in the tests conducted with the largest observed in test 3 and smallest in test 1 corresponding to crack growth from 11 mm- 20 mm and 12 mm- 17 mm respectively. However, in all three tests the peak of AE hit rate was at about crack lengths of 15 mm with ΔK approximately 13 MPa $m^{1/2}$. The region of stage 2 where little or no emissions are produced was about half of those reported by Daniel et al. and Han et al. The reason for this disparity is not apparent but may be attributed to differences in test sample materials and geometry.

With no emissions detected prior to the emergence of the crack in these tests, the detected AE are associated with crack growth only. The observed changes in emission rate must therefore be associated with different aspects of crack growth through the sample. As in the first 3 tests the emissions at 12-15 mm crack length occurred in the lower half of the load cycle, they may be associated with crack closure, which can be expected to change with increased crack length and altered sample geometry.

Such intermittent emission of AE would have clear implications of reduced opportunity for fatigue crack detection in practical applications of the technique as a route to crack detection in structural health monitoring systems. The reappearance of the emissions in stage 3, after a prolonged absence in stage 2, was for a very short period of the samples fatigue life and fatigue crack detection in such instances may be useless as it most likely would not allow for sufficient time to react in terms of maintenance actions.

Future work will focus on characterisation of AE from fatigue crack in various specimens of different physical geometry and also derivation of resulting POD and POL curves.

CONCLUSIONS

- Rates of AE emission from fatigue cracks in nominally identical SEN samples of 2014 T6 subjected to constant amplitude loading vary by a factor of between 6-7
- In all three samples under constant amplitude loading, emissions per mm of crack length were initially small, reached a maximum at approximately 11-15

mm and declined to almost zero at crack lengths greater than 20 mm and remained constant until failure crack length was approached. An increase occurred just prior to failure.
- The majority of emissions at early crack lengths occurred at about the middle and lower portions of the loading range which suggests that they may be associated with crack closure.

ACKNOWLEDGEMENT

This study is sponsored by the Cranfield University IVHM Centre

REFERENCES

[1] Scala, C. M. and Cousland, S. M. (1983), "Acoustic emission during fatigue crack propagation in the aluminium alloys 2024 and 2124", *Materials Science and Engineering*, vol. 61, no. 3, pp. 211-218.

[2] Scruby, C. B., Baldwin, G. R. and Stacey, K. A. (1985), "Characterisation of fatigue crack extension by quantitative acoustic emission", *International Journal of Fracture,* vol. 28, no. 4, pp. 201-222.

[3] Cousland, S. M. and Scala, C. M. (1983), "Acoustic emission during the plastic deformation of aluminium alloys 2024 and 2124", *Materials Science and Engineering*, vol. 57, no. 1, pp. 23-29.

[4] McBride, S. L., MacLachlan, J. W. and Paradis, B. P. (1981), "Acoustic emission and inclusion fracture in 7075 aluminum alloys", *Journal of Nondestructive Evaluation,* vol. 2, no. 1, pp. 35-41.

[5] Scruby, C., Wadley, H. and Sinclair, J. E. (1981), "Origin of Acoustic Emission During Deformation of Aluminium and Aluminium-Magnesium Alloy", *Philosophical Magazine A: Physics of Condensed Matter, Structure, Defects and Mechanical Properties,* vol. 44, no. 2, pp. 249-274.

[6] Meriaux, J., Boinet, M., Fouvry, S. and Lenain, J. C. (2010), "Identification of fretting fatigue crack propagation mechanisms using acoustic emission", *Tribology International,* vol. 43, no. 11, pp. 2166-2174.

[7] Botev, Z.I., Grotowski, J.F. and Kroese, D.P., (2010), *Kernel Density Estimation via Difussion,* Institute of Mathematical Statistics.

[8] Han, Z., Luo, H., Cao, J. and Wang, H. (2011), "Acoustic emission during fatigue crack propagation in a micro-alloyed steel and welds", *Materials Science and Engineering A,* vol. 528, no. 25-26, pp. 7751-7756.

[9] Daniel, I. M., Luo, J. -., Sifniotopoulos, C. G. and Chun, H. -. (1998), "Acoustic emission monitoring of fatigue damage in metals", *Nondestructive Testing and Evaluation,* vol. 14, no. 1-2, pp. 71-87.

[10] Lugo, M., Jordon, J. B., Horstemeyer, M. F., Tschopp, M. A., Harris, J. and Gokhale, A. M. (2011), "Quantification of damage evolution in a 7075 aluminum alloy using an acoustic emission technique", *Materials Science and Engineering A*, vol. 528, no. 22-23, pp. 6708-6714.